ELSEVIER

Chemical Engineering Journal 77 (2000) 19–25

Chemical Engineering Journal

www.elsevier.com/locate/cej

Application of gamma camera imaging and SPECT systems in chemical processes

Apostolos Kantzas [a,b,*], Kelly Hamilton [a,b], Taghi Zarabi [a], Amit Bhargava [a], Ian Wright [a], Glen Brook [a], Jinwen Chen [a,b]

[a] *Department of Chemical and Petroleum Engineering, University of Calgary, Calgary, Alberta, Canada T2N 1N4*
[b] *Tomographic Imaging and Porous Media Laboratory, Calgary, Alberta, Canada*

Abstract

SPECT imaging systems are used in nuclear medicine for diagnostic imaging of heart, brain, lung and other organ functions. Radio-pharmaceuticals are injected in the blood stream of a patient. The propagation of the radio-pharmaceutical is monitored as a function of position and time using a gamma camera. In many tests, the monitoring occurs in real time. This technique has been extended for use in chemical process monitoring in our laboratory. In particular, a Siemens gamma camera with SPECT capabilities is routinely used for real time tracer studies, radioactive particle tracking and SPECT imaging. The same radio-pharmaceuticals used in medical testing are used for process monitoring. The system has been used in determining hydrodynamic properties of gas/solid and liquid/solid fluidized beds and in visualizing and monitoring of multi-phase flow phenomena in porous media. ©2000 Elsevier Science S.A. All rights reserved.

Keywords: Gamma camera; SPECT imaging; Chemical processes; Flow imaging

1. Introduction

Nuclear medicine originated from many scientific discoveries, most notably the discovery of X-rays in 1895 and the discovery of 'artificial radioactivity' in 1934. Wide-spread clinical use of nuclear medicine, however, did not start until the early 1950s. The value of radioactive iodine became apparent as its use increased to measure the function of the thyroid gland and to diagnose thyroid disease. Moreover, the ability to treat a disease with radio-pharmaceuticals and to record and make a picture of the form and structure of an organ was invaluable. The advances in nuclear medicine technology and instrument manufacturers were critical to this development. The 1980s brought the development of cutting-edge nuclear medicine cameras and computers. The gamma camera was brought into a new dimension of imaging with its introduction into the industrial field. For many engineering applications, this apparatus has been shown to be excellent for observation of flow and mixing in reactor vessels [1], for the measurement of liquid film thickness on the surface of a rotating disk [2], for the characterization of cross flow in multi-channel mixing assemblies [3], and for imaging oil displacement in thin slabs of porous media [4].

Presently, radioactive particle tracking seems to offer the most promise for measurement of recirculating phase velocities in gas-fluidized beds and bubble columns. The early work on this technique [5] led only to qualitative results. Jones et al. [6] developed a technique for tracking particle motion in liquids. Due to lack of adequate instrumentation and data acquisition systems, they were unable to obtain good accuracy and resolution. The first of the new generation particle tracking techniques was introduced by Lin et al. [7]. The new generation of particle tracking features a tracer particle that closely matches the physical characteristics of the particles and a series of photo-multiplier tubes placed around the column which detect particle movement.

There are other research-groups that have done extensive work with radioactive particle tracking in multi-phase reactors. Professor Dudukovic's group (Washington University in St. Louis) is using computer automated radioactive particle tracking (CARPT) to study flow pattern, turbulence and mixing in bubble/slurry bubble columns and liquid–solid risers [8–11]. Professor Chaouki's group (Ecole Polytechnique) is focusing on the fluid dynamic properties in three phase fluidized beds using radioactive particle tracking (RPT) [12,13]. Both groups employ single radioactive particle and a number of dispersed scintillation detectors to obtain the trajectories of the labeled particle.

Mann et al. [14] developed a flow model that makes use of an overall circulation structure of velocities to represent the average flow of the fluid in a stirred vessel. The model can provide the frequency of occurrence a radio-pill flow-follower at each cell in the vessel. Convection and

* Corresponding author.
E-mail address: akantzas@ucalgary.ca (A. Kantzas).

PII: S1385-8947(99)00148-5

stochastic turbulence in the vessel can then be quantified. Since the number of particle occurrences is known for each of the cell from RPT experiments, a similar method can be used to evaluate the convection and stochastic turbulence in gas fluidized beds.

Nuclear technology has been utilized in flow studies as well. Lien et al. [15] used a nuclear imaging technique for studying multiphase flow in a porous medium. With this technique, the dynamics of the fluid saturation distributions are recorded. The fluid phases are labeled with nuclear tracers (the brine with either ^{22}NaCl or ^{137}CsCl and the oil phase with ferrocene which has the Fe-ion replaced with the radioisotope ^{59}Fe) and detecting the gamma radiation by a movable germanium detector. A different approach was applied to oil relative permeability determination during a tertiary-gas gravity-drainage experiment by Chalier et al. [16]. With this method, the source, which contains two sealed radioactive sources (^{241}Am and ^{137}Cs), and detector blocks move together along the core measuring gamma ray absorption. Using this technique, it was possible to visualize the fluid saturation distribution in the core as a function of the volume of gas injected.

In this paper, the next generation of particle tracking is presented along with a technique for monitoring the flow of a tracer in a porous medium.

2. Experimental

2.1. Gamma camera systems

There are a number of different types of gamma cameras available but the principle of operation remains the same. The model available in our laboratory is a Siemens Orbiter which has 75 photo-multiplier tubes (PMTs) and a NaI(Tl) crystal with a diameter of 41 cm. The gamma camera (Fig. 1) is designed to detect gamma radiation. The gamma rays originate from a radio-pharmaceutical which, in nuclear medical imaging, is administered directly to the patient and localizes in the organ of interest. The camera has the ability to detect the distribution of radioactivity. This is accomplished by recording the emissions from the radioactivity with an external radiation detector placed outside the area of interest [17].

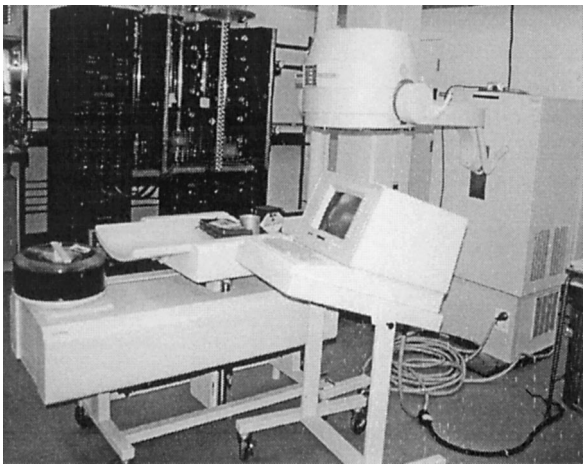

Fig. 1. The Siemens Orbiter System used in this work.

A gamma ray image is projected by the collimator onto the NaI(Tl) detector crystal, creating a pattern of scintillations in the crystal that outlines the distribution of radioactivity in front of the collimator. An array of PMTs viewing the back surface of the crystal, and electronic position logic circuits, determine the location of each scintillation event as it occurs in the crystal. Individual events also are analyzed for energy by pulse-height analyzer circuits. When an event falls within the selected energy window, the electron beam in a cathode ray tube (CRT) display is deflected by *x*- and *y*-position signals to a location on the CRT face corresponding to the location at which the scintillation event occurred in the crystal, and the beam is turned on momentarily, causing a flash of light to appear at that point on the display. Therefore, the CRT display shows a pattern of light flashes corresponding to the pattern of scintillation events occurring in the detector crystal [17].

The gamma camera is capable of producing different types of images: static; dynamic; and single photon emission computed tomography (SPECT). In static imaging studies, an image of an unchanging distribution of radioactivity can be recorded over an extended imaging time. It can be used for dynamic imaging studies in which changes in the distribution of radiation can be observed. As soon as the acquisition of the first frame is complete, it immediately begins to collect a second image on the next frame and so on until the desired number of frames is reached. The images produced with these two methods of acquisition are two-dimensional and can be either recorded directly onto film or acquired and stored by a computer. Some software packages also have the ability to generate three-dimensional images from a dynamic series. True three-dimensional images can be produced using SPECT imaging. With this type of acquisition, the head of the camera physically orbits the object of interest taking a series of static images at different angles. Reconstruction algorithms are used to assimilate all the two-dimensional images and reconstruct them into three-dimensional images from which tomographic slices can be made at any level and in any direction [18]. There are a variety of medical imaging software packages on the market. The software available in our laboratory is Macintosh NucLear Power (NucLear MAC) [19].

The NucLear MAC gamma camera computer is a high performance system for acquisition, display and processing of nuclear medicine images. It provides the performance expected from modern nuclear computers, but with the ease-of-use associated with the Macintosh II family of computers. The software follows the standard Macintosh user interface guidelines. It operates through the familiar menus, windows, mouse controls, and dialog boxes. The NucLear MAC supports the standard image formats of the

Macintosh (PICT, TIFF), so images can be displayed using other standard programs.

The output from the gamma camera is analog and must therefore be converted to a digital form by an analog to digital converter (ADC). After the x (horizontal) and z (vertical) position signals of the gamma camera are digitized, their position values are used to generate images. This is achieved by storing the x and z values in a buffer (500 counts) on the interface board and are then stored in computer memory. After a certain number of these pairs of values are stored, they are read from memory and used to update the image. Each pair represents a location on the image, and when a particular pair is read, the brightness of the pixel at the corresponding position is increased by one. One thousand to 10 000 points are stored in memory between image updates. Because this amount of data buffering represents only a second or two, the images appear to form in nearly real time. This process is performed until a desired number of counts or total acquisition time is reached.

The radio-pharmaceuticals have one or more atoms in the molecular structure which are unstable. This instability results in the emission of gamma particles originating within the molecule. Radio-pharmaceutical agents may be in the form of a solid, liquid, or gas. Depending upon their indicated use and dose form, radio-pharmaceutical agents may be swallowed, inhaled, injected or instilled [18].

Technetium (^{99m}Tc) is the most common radioisotope used in nuclear medicine. It emits 140 keV photons and has a short physical half life of 6.02 h. A radio-nuclide generator system is used to produce the ^{99m}Tc in an aqueous form, sodium pertechnetate ($Na^{99m}TcO_4^-$). In this form, it can be used on its own or attached to a variety of chelating agents to produced a number of different types of radio-pharmaceutical products.

2.2. Chemical reactor engineering applications

The application of radio-pharmaceuticals for radioactive particle tracking offers many advantages including low half-life (in the order of a few hours), ease of handling and disposal and use of available hardware for data acquisition and processing. The gamma camera acquires images of the sample under study at frequencies that can be as high as 1 kHz. In the experiments presented in this paper frequencies up to 50 Hz were attempted. The particle position in each image is easily calculated and the velocity of the particle is calculated from the change of the particle position in two subsequent images. Currently, the particle tracking system is 2-D but improvements towards a 3-D system are under way. The 3-D system under construction is a compilation of two similar cameras positioned at 90° with respect to each other and programmed to acquire data simultaneously.

^{99m}Tc was the radioisotope of choice because of its availability, cost effectiveness, energy of emission and short physical half life. Macroaggregated albumin (MAA), a human serum protein which is conventionally used in lung perfusion imaging, was chosen to chelate to ^{99m}Tc because of its size range of 10–150 μm (90% of those being between 10–70 μm). These particles are small enough to incorporate into a polyethylene particle of 1 mm in size. The radio-labeled protein was separated from the aqueous phase by allowing it to settle and the supernatant was then decanted. With the radioactive protein isolated, a small amount of polyethylene particles were added. Heating the mixture over a Bunsen burner allowed a molten radioactive plastic pellet to form. From this pellet, a particle of radioactive polyethylene was cut to 1 mm in size and yielded ≈1000–1500 counts per second (cps) at the camera face.

The radio-labeled particle, which has the same physical characteristics, i.e., size and density, as the solid phase, was introduced into a laboratory model of a gas fluidized bed. The unit, 1 m in height and 10 cm in diameter, is constructed from Plexiglas and consists of an air supply system, a rotameter, and stainless-steel porous plate distributor. The camera is positioned facing the column and is aligned to image the bottom third of the column which is filled with polyethylene to the desired bed height. With the radioactive polyethylene particle added to it, the bed was fluidized to the desired level. A number of experiments were conducted at minimum fluidization velocity (u_{mf}), at $1.2u_{mf}$ and $1.5u_{mf}$, while bed heights of 10 and 20 cm were used. Data was acquired with matrix sizes of 128×128 and 160×160, frame durations of 20, 50, 100 and 1000 ms. The number of frames acquired per scan ranged from 200 to 1000. Several of these short scans were conducted over a period of 3–4 h for each experimental run.

The series of images collected in each set of experiments (up to several thousand images per experiment) were stored in memory and were transferred to a workstation for further analysis. Each image was processed and the number of counts per pixel was found. Background radiation was subtracted and the scattering around the particle was eliminated. The centre of the radioactive particle was calculated through a center of mass calculation. When this was done the coordinates of the particle were recorded. From the particle coordinates in subsequent frames the velocity of the particle was also calculated. When all the coordinates and all the velocities were calculated, the results were tabulated and plotted using spreadsheets. Furthermore, the data provided frequency distributions for velocity components and probability density functions for the particle location within the column. Additional calculations can be performed to provide local time averaged velocities, azimuthally averaged velocities, fluctuating velocities, intensity of turbulence terms, normal and shear stress terms, turbulent kinetic energy and turbulent dispersion coefficients.

2.3. Flow in porous media applications

In addition to the above experiments, liquid tracer studies have been performed to monitor two phase flow in porous

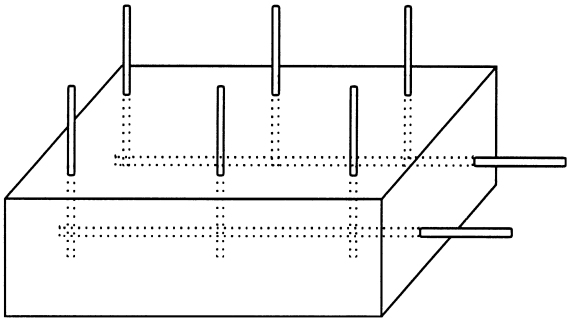

Fig. 2. Schematic of the physical model used in the porous media displacement experiments.

media. The gamma camera system has been used to investigate techniques for the recovery of heavy oil. The camera allowed for the visualization of two phase immiscible displacements in porous media. Brine was labeled with sodium pertechnetate and it was pumped under pressure into a physical model of a heavy oil formation. Experiments were conducted in physical models with rectangular geometry and multiple wells for injecting and producing fluids. Two models were used. The internal dimensions of Model #1 were 50 cm × 30 cm × 10.5 cm and the dimensions of Model #2 were 50 cm × 30 cm × 5 cm. A typical schematic is shown in Fig. 2. The models were wet packed with sand and saturated with brine. The brine was then displaced with heavy oil providing initial oil saturation for the experiments. Static images were acquired at various intervals over a period of several hours to visualize the flow of brine in the porous medium. The recovery techniques investigated included water flooding, and flooding with a water soluble polyacrylamide polymer. Prior to the start of a flood, the aqueous phase would be doped with ^{99m}Tc, with ≈25 mCi of activity being added to 3.5 l of brine or polymer solution. During the displacement the camera would acquire images of the sand. The camera would detect the activity in the aqueous phase and the sweep efficiency of the flood could be determined. Due to the size, it was necessary to acquire three images and then combine them in order to obtain an image of the entire model.

3. Typical results

3.1. Chemical reactor engineering applications

The polyethylene experiments conducted, produced a series of images which can be displayed in individual frames format, cine format or in three dimensions. These images showed good contrast. The particle had sufficient counts to penetrate surrounding media and it was easily distinguishable from the background radiation. A detailed analysis of the experiments has been conducted. A resolution of 3.2 mm has been obtained and particle velocities of up to 4.0 m/s have been calculated.

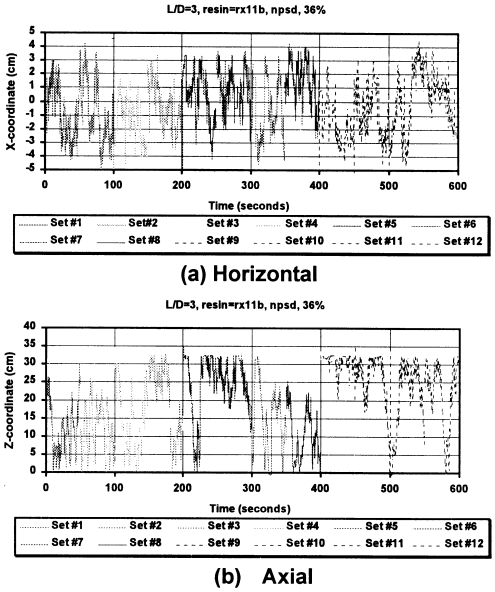

Fig. 3. Determination of particle trajectories in a laboratory scale air/polyethylene fluid bed using radioactive particle tracking.

Figs. 3–5 show some typical results obtained from radioactive particle tracking experiments in a laboratory air/polyethylene fluidized bed. The data shown in this paper is two dimensional in nature since only one gamma camera was used in the experiments. The total sampling time (12 sets) was 10 min with each set lasting 50 s. Since these 12 sets of data were collected over 1 h of experimental time, the results should represent the time averaged quantities in the bed. Fig. 3(a) and (b) display the particle trajectories in horizontal and axial directions, respectively. It is seen that the particle is traveling everywhere in the bed, indicating a good mixing of solids phase.

Fig. 4 shows the probability distribution function (PDF) of particle occurrence in the bed at the same conditions as discussed above. This plot was obtained by dividing the bed into many compartments and counting the number of particle occurrences (particle visiting times) in each compartment.

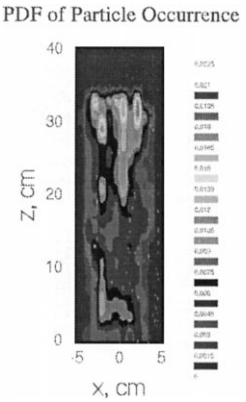

Fig. 4. Probability distribution function (PDF) of particle occurrence in the bed.

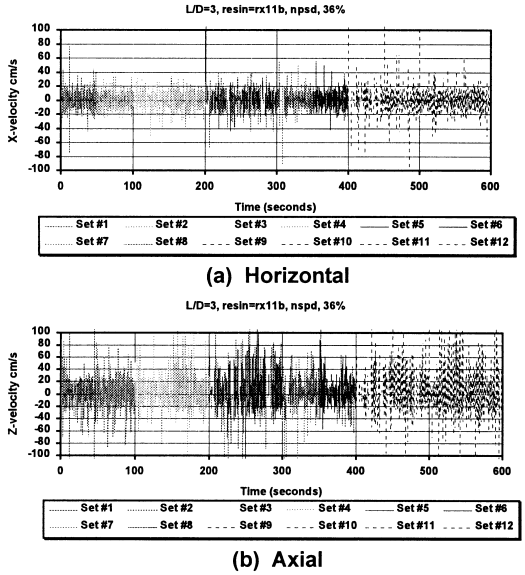

Fig. 5. Determination of particle velocity components in a laboratory scale air/polyethylene fluid bed using radioactive particle tracking.

It is clear that the particle visited everywhere in the bed. In the top part of the bed, the PDF of particle occurrence seems higher than in the bottom part, meaning that the particle stayed longer in this part.

Fig. 5(a) and (b) show the horizontal and axial velocity components of the particle, respectively, at the same conditions. The horizontal velocity is oscillating in the range of −40 to 40 cm/s. Compared to the horizontal velocity, the axial velocity is fluctuating in a wider range, from −100 to 100 cm/s. This is understandable since the motion of the solids in gas fluidized beds is axially dominant. Both of the horizontal and axial velocity components show no particular trends in radial direction since the bed is essentially in bubbly flow regime, in which gas voidage is expected to be uniformly distributed in the cross section of the bed. This is to be confirmed by CT scanning, although similar tests on similar resins showed radial variability of voidage [20].

3.2. Flow in porous media applications

Physical models shown in Fig. 2 were used for the tracer experiments. The heavy oil saturated model was flooded by brine. The doped brine was injected from the three wells at the front of the model. The camera acquired a series of images such as the one shown in Fig. 6. The image in this figure shows the brine swept area at the end of the waterflood. The scale is in counts per pixel. The injectors are in the bottom of the image and the producers are in the top of the image. They are seen as dark (blue) points at the center and edges of the bottom and top of the image respectively. The bright (yellow and red) stream-like areas of the image are the areas swept by the injection phase. The dark point at the center of the image is a bolt used to hold

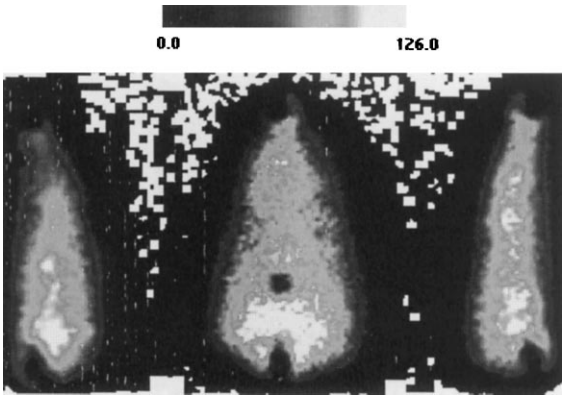

Fig. 6. Gamma-camera imaging of the displacement of heavy oil by brine. Visualization of sweep efficiency.

the model together. The black and white area in between the wells corresponds to the area of poorly swept reservoir.

4. Discussion

4.1. Chemical reactor engineering applications

The particle trajectory values obtained in the experiments with polyethylene resins revealed valuable information. With each experiment, a series of graphs similar to those of Figs. 3–5 are obtained. From such figures and especially the figures similar to Fig. 4, a number of observations can be made. For the same type of resin, and the same range of dimensionless velocities (u/u_{mf}) it was found that the particle size distribution and the gas velocity affect greatly the probability distribution function of particle location. It was found that the particle generally stays away from the column wall. In a number of instances, the particle seems to be 'stuck' in a very small location in the column ($\approx$1 cm^3) for time periods of several seconds. Each 1000 frame data set at 50 ms per frame yields a time duration per data set of 50 s. There is a gap of several minutes in between subsequent tests and the results revealed that the particle can be 'stuck' for several minutes. This observation is made at lower flow rates. As gas velocity increases, the particle covers larger portions of the bed.

In several tests, the particle seems to be immobile for an extended period of time and then 'jumps' to a new location and starts moving in an extended part of the bed. Some other times the opposite is observed. The particle is moving freely for an extended period of time and then it seems to get 'stuck'. Such flow patterns indicate that there are several regions in the bed that correspond to different flow domains within the column. This speculation is currently under further investigation.

Figs. 7 and 8 show some comparisons of horizontal (x-direction) position profiles for a set of six experiments at similar flow rates. One group of experiments is done with a wide particle size distribution resin while the second

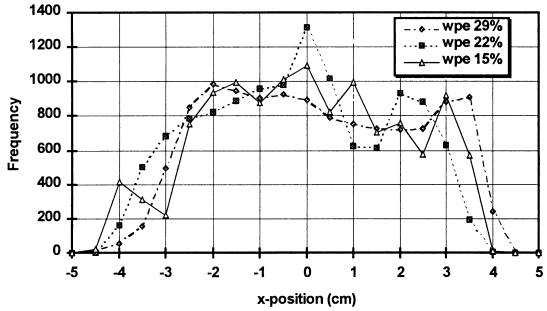

Fig. 7. Horizontal position profiles for a series of experiments using wide particle size distribution polyethylene.

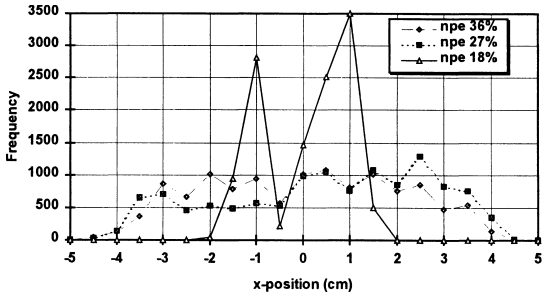

Fig. 8. Horizontal position profiles for a series of experiments using narrow particle size distribution polyethylene.

group of experiments is done with a narrow particle size distribution sample from the same resin. The wide particle size distribution resin profiles are almost parabolic in shape and almost symmetrical.

In Fig. 8, the profiles for low flow rates are much narrower than the same profiles for higher rates. Comparison of the two figures indicates that with the wider size distribution better mixing is achieved through the whole horizontal distance.

Figs. 9 and 10 show the axial (*z*-direction) profiles for the same experiments as in Figs. 7 and 8. In Fig. 9, it is clearly shown that the radioactive particle moves at the top two-thirds of the column and it never reaches the bottom part of the column for any of the experiments. Such patterns indicate circulating mixing zones that cover only parts of the bed.

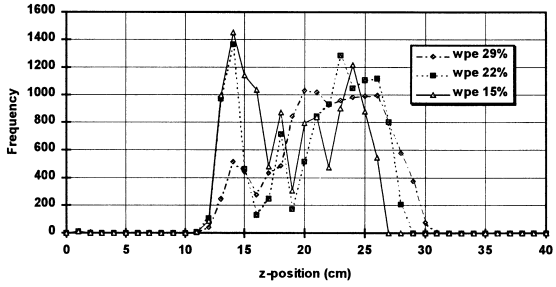

Fig. 9. Axial position profiles for a series of experiments using wide particle size distribution polyethylene.

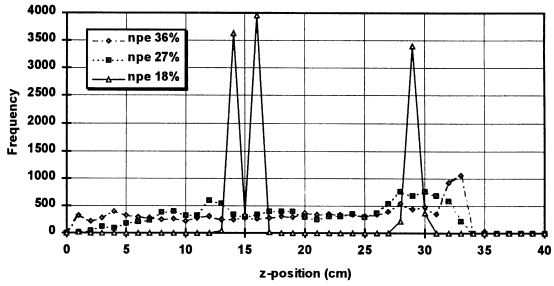

Fig. 10. Axial position profiles for a series of experiments using narrow particle size distribution polyethylene.

The picture is quite different for the narrow particle distribution data. For the low rate, the particle remains stagnant in specific locations. For the higher rates, however the particle moves through the whole length of the column although it seems to be spending relatively more time at the top part of the column 'tumbling' at the bed surface. This type of behaviour is currently under further investigation.

Although the data acquisition process is only two-dimensional, the collected data never revealed radial symmetry. This observation contradicts the common assumption that radial symmetry is expected to exist in fluid bed columns and that those 2-D measurements can be extrapolated to 3-D predictions. Whether this observation is due to the number of data collected or it is indeed the true representation of the flow behaviour is currently under investigation.

With the recent acquisition of a second gamma camera, a Siemens ZLC 7500, location of the particle in the *y*-direction will be obtained when the camera is positioned at 90° to the currently used gamma camera.

4.2. Flow in porous media applications

The displacement of a viscous fluid by a much less viscous displacing fluid (such as the waterflood of heavy oil formation) leads to instabilities that are generally called 'viscous fingering', and result in poor sweep efficiency. Linear core flooding experiments cannot provide useful information on these phenomena because they are linear displacement experiments. Numerical simulation of displacement processes provides predictions of area sweep efficiency for any displacement process, but validation through experimental work is not readily available. Experiments such as the ones presented here offer this validation capability for laboratory scale experiments and allow for the tuning of simulation tools.

With respect to the transformation of the images from displacements in porous media into actual fluid saturation maps, the work is in progress. The main obstacle is the accurate determination of the activity of the tracer inside the porous medium and the possible interactions between the tracer and other matter that lies in front of the camera such as the walls of the physical model. Detailed calibration experiments are under way to solve this problem.

The same liquid tracer technology that was applied to the heavy oil experiments discussed above has been used to determine the flow paths in native state soil samples. Furthermore, tracer studies of liquid flow in liquid–solid fluidized beds were performed, while in the same systems radioactive particle tracking of the solid phase was also attempted. Troubleshooting tests revealed that applications of this technology also lie with the pulp and paper, biological, and food industries.

5. Conclusions

The experiments presented in this paper demonstrate the effectiveness of the gamma camera as a tool in the field of chemical and petroleum engineering. Applications of this technique were demonstrated through two examples:

1. Radioactive particle tracking in fluidized beds. Polyethylene particles were tagged and their trajectories and velocities (x- and z-components) were calculated in laboratory scale air-polyethylene fluidized beds. The results are promising. High and low solid velocity regions and high and low mixing areas were identified and monitored as a function of superficial gas velocity and particle size distribution.
2. Radioactive tracer studies were performed in laboratory scale physical models that emulate heavy oil reservoirs. The tracer revealed the flow paths of water displacing oil, identified viscous fingering and qualitatively described sweep efficiency.

Acknowledgements

This research was made possible through funding by Nova Chemicals, Trojan Technologies, the Alberta Department of Energy and the Natural Sciences and Engineering Research Council of Canada. A special thank you goes out to Dr. L. Hahn for initiating access to ^{99m}Tc from Foothills Medical Center, Calgary, to Ingrid Koslowsky for her invaluable advice and for providing the radioactive materials, and to Barry Gulck for the preparation of the radioactive materials.

References

[1] F.S. Castellana, M.I. Friedman, J.L. Spencer, Characterization of mixing in reactor through analysis of regional tracer dilution data obtained with gamma camera, AIChE J. 26 (1984) 207–213.
[2] F.S. Castellana, R.H. Hsu, Measurement of liquid film thickness on the surface of a partially immersed vertical rotating disc using a gamma camera, Chem. Eng. Commun. 26 (1984) 111–115.
[3] R.H. Hsu, Characterization of Mixing in Multi-Channel Crossflow Mixing Assemblies, PhD dissertation, Columbia U., New York City, 1984.
[4] Y.B. Huang, C.C. Gryte, Gamma camera imaging of oil displacement in thin slabs of porous media, J. Petrol. Tech. 40 (1988) 1355–1360.
[5] N.B. Kodukov, A.N. Kornilaev, I.M. Skachko, A.A. Akhromenkov, A.S. Kurglov, An investigation of the parameters of moving particles in a fluidized bed by a radioisotopic method, Int. Chem. Eng. 4 (1964) 43–47.
[6] B.C. Jones, B.T. Chao, M.A. Shirazi, An experimental study of the motion of small particles in a turbulent fluid field using digital techniques for statistical data processing, Dev. Mech. 4 (1968) 1249–1255.
[7] J.S. Lin, M.M. Chen, B.T. Chao, A novel radioactive particle tracking facility for measurement of solids motion in gas fluidized beds, AIChE J. 31 (1985) 465–473.
[8] N. Devanathan, D. Moslemian, M.P. Duduković, Flow mapping in bubble columns using CARPT, Chem. Eng. Sci. 45 (1990) 2285–2291.
[9] Y.B. Yang, N. Devanathan, M.P. Duduković, Liquid backmixing in bubble columns via computer-automated radioactive particle tracking (CARPT), Exp. Fluids 16 (1992) 1–9.
[10] S. Roy, J. Chen, S. Kumar, M.H. Al-Dahhan, M.P. Duduković, Tomography and particle tracking studies in a liquid–solid riser, Ind. Eng. Chem. Res. 36 (11) (1997) 4666–4669.
[11] J. Chen, F. Li, S. Degaleesan, P. Gupta, M.H. Al-Dahhan, M.P. Duduković, B.A. Toseland, Fluid dynamic parameters in bubble columns with internals, Chem. Eng. Sci. 54 (13-14) (1999) 2187–2197.
[12] F. Larachi, G. Kennedy, J. Chaouki, 3-D Mapping of solids flow fields in multiphase reactors with RPT, AIChE J. 41 (2) (1995) 439–443.
[13] F. Larachi, M. Cassanello, J. Chaouki, C. Guy, Flow structure of the solids in a three-dimensional gas–liquid–solid fluidized beds, AIChE J. 42 (9) (1996) 2439–2452.
[14] R. Maan, P.P. Mavros, J.C. Middleton, A structured stochastic flow model for interpreting flow-follower data from a stirred vessel, Trans. Inst. Chem. Eng. 59 (1981) 171–278.
[15] J.R. Lien, A. Graue, K. Kolltveit, A nuclear imaging technique for studying multiphase flow in a porous medium at oil reservoir conditions, Nucl. Inst. Methods A271 (1988) 693–700.
[16] G. Chalier, S. Sakthikumar, V. Guiry, P. Maquignon, Dual Energy Gamma-Ray Absorption Technique Applied to Oil Relative Permeability Determination During a Tertiary Gas Gravity Drainage Experiment, presented at the International Symposium of the Society of Core Analysts, San Francisco, USA, 1995.
[17] J.A. Sorenson, M.E. Phelps, The anger camera: basic principles, Physics in Nuclear Medicine, W.B. Saunders Co., Philadelphia, PA, 1987, pp. 298–300.
[18] P.J. Early, D.B. Sodee, Computer fundamentals, Principles and Practice of Nuclear Medicine, Mosby-Year Book Inc., St. Louis, MI, 1995, pp. 232–239.
[19] NucLear Mac User Manual v.4/95. Copyright 1985–1995 Scientific Imaging, Inc., pp. A1, C1–C3.
[20] A. Kantzas, I. Wright, N. Kalogerakis, Quantification of channeling in polyethylene resin fluid beds using X-ray computer assisted tomography (CAT), Chem. Eng. Sci. 52 (13) (1997) 2023–2035.